Sonochemical Synthesis of Cadmium(II) Coordination Polymer Nanospheres as Precursor for Cadmium Oxide Nanoparticles

Farhad Akbari Afkhami [1] [ID]**, Ali Akbar Khandar** [1]**, Ghodrat Mahmoudi** [2],* [ID]**, Reza Abdollahi** [3]**, Atash V. Gurbanov** [4,5] **and Alexander M. Kirillov** [5,6],* [ID]

[1] Department of Inorganic Chemistry, Faculty of Chemistry, University of Tabriz, 51666-16471 Tabriz, Iran; f.a.afkhami@gmail.com (F.A.A.); akhandar@yahoo.com (A.A.K.)

[2] Department of Chemistry, Faculty of Science, University of Maragheh, 55181-83111 Maragheh, Iran

[3] Department of Physical Chemistry, Faculty of Chemistry, University of Tabriz, 51666-16471 Tabriz, Iran; chemethod@gmail.com

[4] Department of Organic Chemistry, Baku State University, Z. Khalilov str. 23, AZ 1148 Baku, Azerbaijan; organik10@hotmail.com

[5] Centro de Química Estrutural, Instituto Superior Técnico, Universidade de Lisboa, Av. Rovisco Pais, 1049-001 Lisbon, Portugal

[6] Peoples' Friendship University of Russia (RUDN University), 6 Miklukho-Maklaya st., Moscow 117198, Russia

* Correspondence: ghodratmahmoudi@gmail.com (G.M.); kirillov@tecnico.ulisboa.pt (A.M.K.)

Abstract: Nanospheres of a new coordination polymer $\{[Cd_2(\mu\text{-HL})(\mu\text{-L})(NO_3)_3(H_2O)]\cdot H_2O\}_n$ (**1**) were easily prepared by a sonochemical method from cadmium(II) nitrate and HL (HL, pyridine-2-carboxaldehyde isonicotinoyl hydrazone) in ethanol. Single crystals of **1** were also obtained using a branched tube method. The crystal structure of **1** indicates that the $\mu\text{-HL}/\mu\text{-L}^-$ blocks act as linkers between the Cd(II) centers, assembling them into 1D tooth-shaped interdigitated chains, which are further interlinked into a complex 3D H-bonded network with a rare **hms** (3,5-conn) topology. Nanoparticles of **1** were characterized by elemental analysis, FT-IR spectroscopy, and powder X-ray diffraction (XPRD), while their spherical morphology was confirmed by transmission electron microscopy (TEM). Furthermore, in the presence of a surfactant, the thermolysis of sonochemically generated nanoparticles of **1** led to the formation of cadmium oxide nanospheres (cubic CdO) with an average diameter of 10 nm. This study extends the application of sonochemical synthetic methods for the generation of phase pure nanoparticles of coordination polymers and their thermolysis products.

Keywords: sonochemical synthesis; coordination polymers; metal-organic frameworks; crystal structure; crystal engineering; cadmium; nanoparticles

1. Introduction

Nanoscale materials feature a variety of interesting physical and chemical properties that are primarily affected by their structural characteristics, morphological type, shape and size [1–10]. There is a high diversity of methods for the preparation of nanomaterials [1–3], with notable examples including the microwave-assisted synthesis [11], solvothermal [12], sol-gel [13], and magnetic-field-driven methods [11], as well as microemulsion [14,15], micelle-assisted [16] and cluster growth [17] protocols. Although considerable progress has been made in recent years in the synthetic methodologies for

nanoscale materials, the development of versatile, facile, and inexpensive methods for the preparation of nanocrystalline materials still remains a challenging area of research.

Among a variety of strategies applied for the generation of nanoparticles, the sonochemical synthesis is particularly attractive, given its simplicity, cost effectiveness, quick reaction times, excellent yields, and purity of products [18,19]. Hence, in the past decade, ultrasonic irradiation has been applied for the synthesis of nanoparticles for a wide range of compounds [18–28]. In particular, synthesis of group 12 semiconductor nanoparticles (e.g., CdO, CdS, ZnO, ZnS) is of major interest, due to their size- and shape-dependent electronic and optical properties, as well as potential applications in light-emitting devices and nonlinear optics [29–31]. Cadmium oxide (CdO) is also an important inorganic semiconductor with a large band gap [32].

On the other hand, coordination polymers (CPs) assembled from metal nodes and multidentate organic linkers can be used as precursors for a desirable type of nanoparticles. Such parameters as the composition, size and morphology of metal oxide nanoparticles can be influenced by selecting an appropriate type of metal-organic precursor, and tuning the experimental conditions. Interestingly, nanoscale CPs can also be applied for the preparation of nanomaterials with controlled particle size and uniform morphologies, and eventually more desirable properties [33–36].

Considering all these points, and following our interests in crystal engineering, design of novel coordination polymers and derived functional materials [37–44], we focused our attention on developing a sonochemical synthetic approach for the preparation of a new cadmium(II) coordination polymer as a precursor for nanospheres of CdO. Another objective of this study is to synthesize different forms of Cd(II) CPs, namely nanospheres and single crystals, by exploring the same type of the reaction mixture whilst using distinct synthetic methods (i.e., sonochemical synthesis and branched tube methods, respectively; Scheme 1). Thus, in this study, we report the two different synthetic pathways, crystal structure, topological features, and full characterization of a new 1D coordination polymer {[Cd$_2$(μ-HL)(μ-L)(NO$_3$)$_3$(H$_2$O)]·H$_2$O}$_n$ (**1**), which was assembled from cadmium(II) nitrate and pyridine-2-carboxaldehyde isonicotinoyl hydrazone (HL) in ethanol as a green reaction medium. In addition, the obtained nanospheres of **1** were used for the preparation of CdO nanoparticles with spherical morphology (Scheme 1).
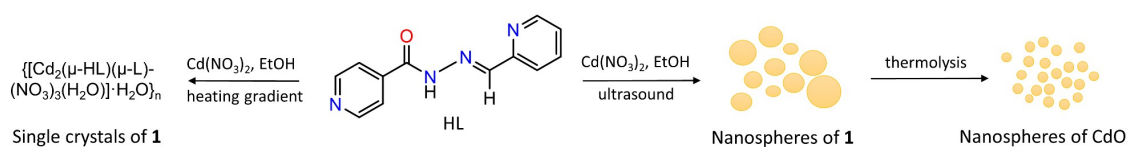
Scheme 1. Synthesis of **1** by sonochemical (nanospheres product form) and branched tube (single crystals product form) methods.

2. Experimental Section

2.1. Materials and Measurements

Unless stated otherwise, all chemicals were obtained from Sigma-Aldrich, and were used as received. Elemental (C, H, N) analyses were performed on a Vario EL III instrument (Ronkonkoma, NY, USA). FT-IR spectra were measured in the 4000-400 cm^{-1} range on a Bruker Tensor 27 FT-IR spectrometer (Bruker Scientific LLC, Billerica, MA, USA) using KBr discs. Powder X-ray powder diffraction (PXRD) patterns were obtained on a STOE type STADY-MP diffractometer (PEYBORD Advanced Laboratory Science Co, Tehran, Iran) using Cu-Kα radiation with λ = 1.5418. Thermogravimetric analysis (TGA) was performed (air atmosphere, 25−800 °C, 10 °C/min) on a NETZSCH STA 449C equipment (Burlington, MA, USA). For ultrasonic irradiation, SONICA-2200 EP ultrasonic bath (Röntgen, Milano, Italy) was applied (40 KHz frequency). Transmission electron microscopy (TEM) images were taken with a JEM-2010 UHR, 200 kV transmission electron microscope

(Peabody, MA, USA). The size of the nanoparticles was estimated from TEM images using the ImageJ software (NIH, Bethesda, MD, USA) [45].

2.2. Structure Determination

Intensity data collection was performed on a Bruker APEX-II CCD diffractometer using single crystals of $\{[Cd_2(\mu\text{-HL})(\mu\text{-L})(NO_3)_3(H_2O)]\cdot H_2O\}_n$ (**1**) and a graphite-monochromated Mo-Kα radiation ($\lambda = 0.71073$ Å). The collected frames were integrated with the Saint software [46] using a narrow-frame algorithm. Data were corrected for absorption effects, using the multi-scan method in SADABS [47]. The space group was assigned using XPREP of the Bruker ShelXTL package. Despite the absence of a chiral center in μ-HL/μ-L$^-$, compound **1** crystallized in a noncentrosymmetric space group P2$_1$. The structure was solved with ShelXT and refined with ShelXL [48,49] and the graphical ShelXle [50] interface. All non-H atoms were refined anisotropically. Hydrogen atoms bonded to C atoms were placed in idealized positions, and their coordinates and thermal parameters were restrained to ride on the carrier atom. With the exception of O1W, hydrogen atoms bonded to N or O atoms were located from the difference map. Their coordinates were allowed to refine freely, while the thermal parameters were constrained to ride on the carrier atom. For the lattice water molecule O1W, hydrogen atoms were placed along ideal hydrogen bond vectors, and restrained to be approximately 0.9 Å from the oxygen atom. After refining them into chemically reasonable positions, their coordinates and thermal parameters were fixed. The assignment of O1W as a water molecule is supported by charge balance and hydrogen bond donor-to-acceptor distances. The structure of **1** was refined as a racemic twin with relative twin fractions of 0.54(3) and 0.46(3). Although the structure was refined in a polar space group, on average, the crystal is not polar. Structural data for **1** are listed in Table 1. Mercury CSD [51] and ToposPro [52,53] software was used for structural and topological representation.

Table 1. Crystal data and structure refinement for compound **1**.

Formula	$C_{24}H_{23}Cd_2N_{11}O_{13}$
Fw	898.33
Crystal system	Monoclinic
Space group	P2$_1$
a (Å)	7.8082(6)
b (Å)	14.9024(9)
c (Å)	13.4584(10)
α (º)	90.00
β (º)	98.903(2)
γ (º)	90.00
V (Å^3)	1547.16(19)
Temp (K)	100(2)
Z	2
D_c(g.cm^{-3})	1.928
μ(mm^{-1})	1.459
Index ranges	$-9 < h < 9$
	$-19 < h < 19$
	$-17 < h < 17$
F(000)	888
R_{int}	0.0290
R_1 (I > 2σ(I))	0.0388
wR (all data)	0.0708
GOF	0.985

2.3. Topological Analysis

Topological analysis of the 1D coordination polymer **1** and its 3D H-bonded network was performed with ToposPro by applying a concept of the underlying (simplified) net [52,53]. A simplified 1D coordination network was obtained by omitting the terminal ligands and contracting the bridging

ligands to the respective centroids. A simplified 3D H-bonded net was generated by contracting the [Cd(L)(NO$_3$)(H$_2$O)] and [Cd(HL)(NO$_3$)$_2$] blocks to centroids, maintaining their connectivity via coordination and hydrogen bonds. Only strong H-bonds (D-H···A) were taken into account, with the H···A < 2.50 Å, D···A < 3.50 Å, and ∠(D−H···A) > 120°; D and A refer to donor and acceptor atoms [52,53]. For simplicity, crystallization H$_2$O molecules were disregarded in topological analysis. Topological classification of the generated nets was then performed.

2.4. Synthesis of {[Cd$_2$(μ-HL)(μ-L)(NO$_3$)$_3$(H$_2$O)]·H$_2$O}$_n$ (**1**)

HL (pyridine-2-carboxaldehyde isonicotinoyl hydrazone) was prepared according to a literature method [54,55]. A branched tube method [56,57] was used for the synthesis of **1** (Figure S1, in the supplementary materials). Hence, solid Cd(NO$_3$)$_2$·4H$_2$O (0.154 g, 0.5 mmol) and HL (0.113 g, 0.5 mmol) were introduced into the principal arm of a branched tube, followed by a gentle addition of EtOH to fill the arm. The tube was then sealed and immersed in an oil bath with a temperature of 60 °C, whereas the branched (cooler) arm was kept at ambient temperature. A good amount of single crystals was formed in the cooler arm in 3 days. These were isolated manually and dried in air to give compound **1** (single crystals form). Yield: 72% (based on cadmium(II) nitrate). Anal. Calcd. for C$_{24}$H$_{23}$Cd$_2$N$_{11}$O$_{13}$: C, 32.09; H, 2.58; N, 17.15. Found: C, 32.33; H, 2.66; N: 17.04%. FT-IR data (cm^{-1}): Selected bands: 3436, 3193, 2096, 1992, 1647, 1512, 1462, 1435, 1342, 1290, 1224, 1157, 1091, 1041, 924, 813, 741, 701, 633.

2.5. Synthesis of {[Cd$_2$(μ-HL)(μ-L)(NO$_3$)$_3$(H$_2$O)]·H$_2$O}$_n$ (**1**)

Sonochemical synthesis of **1** was carried out in an ultrasonic bath. A solution of Cd(NO$_3$)$_2$·4H$_2$O (0.154 g, 0.5 mmol) in EtOH (10 mL) was added dropwise to a solution of HL (0.113 g, 0.5 mmol) in EtOH (10 mL). The obtained mixture was treated at ambient temperature in the ultrasonic bath for 30 min, resulting in a generation of yellow solid. This was filtered off, washed with ethanol, and dried in air to furnish nanoparticles of **1**. Yield: 76% (based on cadmium(II) nitrate). Anal. Calcd. for C$_{24}$H$_{23}$Cd$_2$N$_{11}$O$_{13}$: C, 32.09; H, 2.58; N, 17.15. Found: C, 32.20; H, 2.51; N: 17.19%. FT-IR data (cm^{-1}): Selected bands: 3437, 3200, 2116, 1997, 1647, 1513, 1463, 1434, 1342, 1292, 1223, 1156, 1091, 1043, 925, 813, 743, 699, 632.

2.6. Preparation of CdO Nanoparticles

Nanoparticles of compound **1** (0.225 g, 0.25 mmol) and oleylamine (OL, 2.0 g, 7.5 mmol) surfactant were combined in a porcelain crucible. The obtained mixture was heated in a furnace up to 500 °C in air atmosphere and maintained at this temperature for 5 h. After cooling the crucible to ambient temperature, the obtained solid was washed with a small amount of ethanol and acetone to remove any organic residue and dried in air to generate CdO nanoparticles.

3. Results and Discussion

3.1. Synthesis of **1**

Two different synthetic procedures were used for the preparation of a new Cd(II) 1D coordination polymer, {[Cd$_2$(μ-HL)(μ-L)(NO$_3$)$_3$(H$_2$O)]·H$_2$O}$_n$ (**1**), which is driven by the N$_3$O-tetradentate chelating-bridging HL/L$^-$ ligands. These procedures include: (a) a branched tube method with a heat gradient that resulted in a single crystalline form of **1** (Figure S1), and (b) a sonochemical method that led to the formation of nanoparticles of **1**. Both methods are based on a reaction of cadmium(II) nitrate with HL in ethanol (Scheme 1), wherein HL was used as a recognized organic building block for the generation of coordination polymers [54–57].

3.2. Structural and Topological Description of **1**

Compound **1** features a 1D zigzag coordination polymer structure. An asymmetric unit comprises two independent Cd(II) centers, one μ-HL and one μ-L$^-$ linker, three terminal nitrate and one water

ligands, and a H_2O molecule of crystallization (Figure 1). Selected bonding parameters for **1** are given in Table 2. The Cd1 center is eight-coordinate and shows a distorted dodecahedral {CdN_3O_5} geometry (Figure 2A), which is filled by O1, N3 and N4 donors coming from μ-HL block, a N5 donor from μ-L^- linker, and two pairs of O3/O4 and O6/O7 atoms from two bidentate nitrate ligands. In contrast, the Cd2 center is seven-coordinate and reveals a distorted monocapped trigonal-prismatic {CdN_3O_4} geometry (Fig. 2B). Herein, the μ-L^- block acts as an anionic N_2,O-chelating ligand via O2, N7 and N8 donors, and the coordination geometry of Cd2 is completed by a N1 atom from an adjacent μ-HL moiety, as well as by two terminal nitrate O9/O10 atoms, and an H_2O ligand (O12). Given the presence of a pyridine functionality, both the μ-HL/μ-L^- blocks act as the linkers, and lead to the generation of 1D zigzag coordination polymer chains with the 2C1 topology (Figure 3A,B). These chains are interdigitated and show a tooth-shaped pattern.
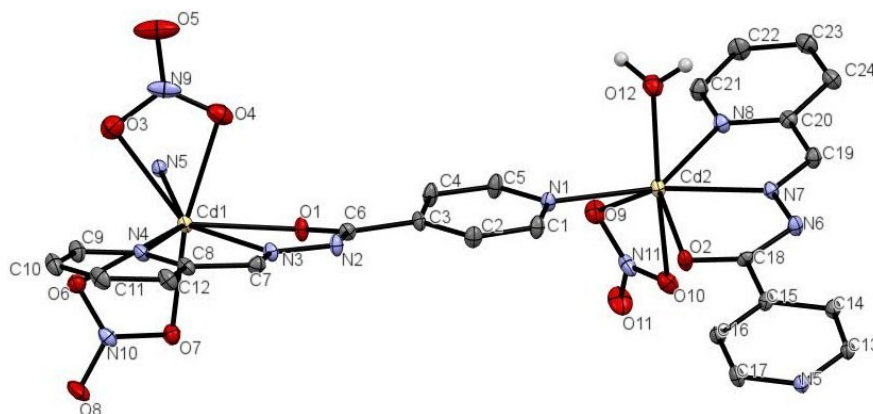

Figure 1. Anisotropic displacement ellipsoid diagram of **1** with a view of coordination environments around Cd1 and Cd2 centers. Thermal ellipsoids are at 30% probability. N5 atom was generated by a symmetry operator ($-1 + x$, $+y$, $-1 + z$).

Table 2. Selected bonding parameters for **1**.

Bond Lengths (Å)		Bond Angles (°)	
Cd1−O3	2.528(4)	O4−Cd1−O3	52.24(13)
Cd1−O4	2.381(4)	O7−Cd1−O6	52.61(11)
Cd1−O6	2.526(3)	N3−Cd1−N4	67.46(12)
Cd1−O7	2.351(4)	N3−Cd1−O1	64.53(10)
Cd1−O1	2.516(3)	N5^i−Cd1−N4	143.21(13)
Cd1−N3	2.373(3)	N5^i−Cd1−N3	145.68(12)
Cd1−N4	2.420(4)	N5^i−Cd1−O1	84.39(12)
Cd1−N5^i	2.317(4)	O10−Cd2−O9	51.38(11)
Cd2−O9	2.585(3)	N7−Cd2−O2	67.33(11)
Cd2−O10	2.384(4)	N7−Cd2−N8	68.76(12)
Cd2−O2	2.360(3)	N1−Cd2−O12	84.23(13)
Cd2−O12	2.341(3)	N1−Cd2−N8	140.20(13)
Cd2−N1	2.341(4)	N1−Cd2−O2	83.81(13)
Cd2−N7	2.308(3)	N1−Cd2−N7	148.30(12)
Cd2−N8	2.467(4)		

^{i} N5 atom was generated by a symmetry operator ($-1 + x$, $+y$, $-1 + z$).

(**A**)   (**B**)
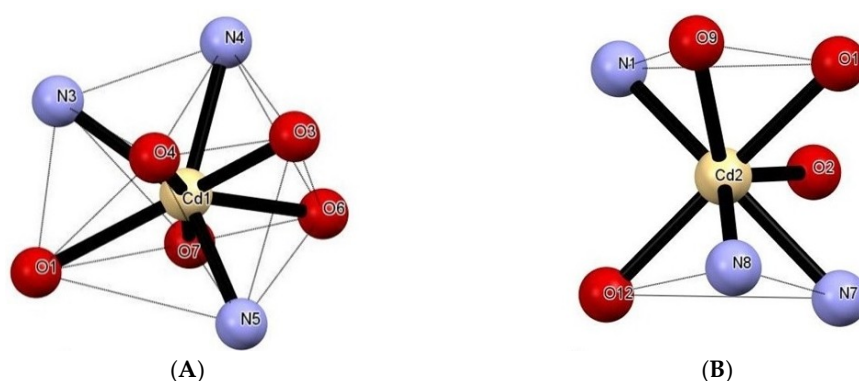
Figure 2. Representation of (**A**) dodecahedral and (**B**) monocapped trigonal-prismatic geometries of Cd1 and Cd2 atoms in **1**.

(**A**)   (**B**)


(**C**)

(**D**)
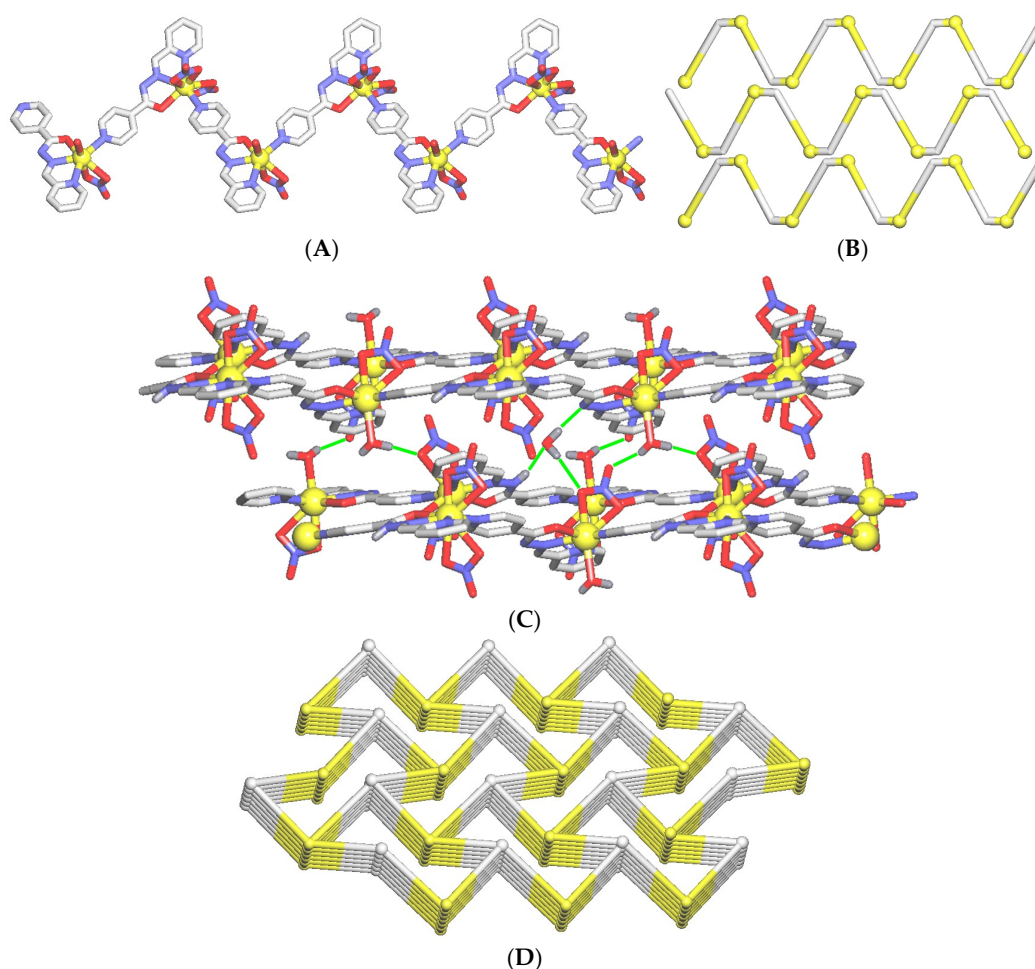
Figure 3. Structural fragments of **1**. (**A**) 1D zig-zag metal-organic chain and (**B**) its topological representation showing three interdigitated chains with the 2C1 topology. (**C**) Interlinkage of 1D chains into a 3D H-bonded network. H-bonds are displayed as green lines (for details see Table S1). (**D**) Topological representation of 3D H-bonded framework showing a binodal 3,5-connected net with the **hms** (3,5-conn) topology and point symbol of $(6^3)(6^9.8)$. Further details: (**A**,**C**) CH hydrogen atoms are omitted, Cd (yellow balls), N (blue), O (red), C (gray); (**B**) Cd nodes (yellow balls), centroids of μ-HL/μ-L$^-$ blocks (gray); (**C**,**D**) views along the *b* (**C**) and *a* (**D**) axis; (**D**) centroids of 3-connected Cd2-based [Cd(L)(NO$_3$)(H$_2$O)] nodes (gray balls), centroids of 5-connected Cd1-based [Cd(HL)(NO$_3$)$_2$] nodes (yellow balls).

In **1**, the μ-HL/μ-L$^-$ ligands have four available coordination sites as a (1,3) set, two coordination poles, one of monodentate, and the other one of tridentate type. Following this strategy, **1** possesses only a C_2 chirality. The non-centrosymmetric character of the compound arises from the presence of two different coordination environments around Cd(II) centres in the asymmetric unit. In Cd1, there are two nitrate ligands, and the μ-HL block contains an N2 atom, whereas in Cd2 there are one nitrate, one water and a deprotonated N6 atom of μ-L$^-$. As the space group $P2_1$ possesses only the C_2 axis of symmetry, this polar space group exhibits the polar direction running parallel to the *b* axis (Figure S4).

The adjacent 1D metal-organic chains are interlinked by strong O−H . . . O, O−H . . . N, and N−H . . . O hydrogen bonds (D···A = 2.687−3.162 Å, Table S1) that also involve the trapped water molecules of crystallization. As a result, a complex 3D H-bonded network is generated (Figure 3C and Figure S4). It was simplified by reducing the Cd2-based [Cd(L)(NO$_3$)(H$_2$O)] and Cd1-based [Cd(HL)(NO$_3$)$_2$] blocks to centroids, and treating them as the 3-connected and 5-connected nodes, respectively (Figure 3D and Figure S3). A standard simplification procedure for H-bonded nets was applied [53,54]. The obtained network can be topologically described as a binodal 3,5-connected net with the **hms** (3,5-conn) topology, and the point symbol of (6^3)(6^9.8). Herein, the (6^3) and (6^9.8) indices refer to the Cd1- and Cd2-based nodes, respectively. It should be mentioned that the present type of topology is rare in coordination compounds [58,59].

3.3. FT-IR and TGA

No significant differences were observed between the elemental analyses, the FT-IR spectra of the single crystals, and nanoparticles of **1**, despite the variation in their preparation methods. Figure 4 shows the FT-IR spectra of the free HL ligand, single crystals and nanoparticles of **1**. A characteristic absorption band corresponding to the C=O stretching vibration of the carbonyl group shifts from 1665 cm^{-1} in HL to 1647 cm^{-1} in both samples of **1**, indicating the coordination of the C=O group to Cd(II) centers. The bands of NO$_3$$^-$ ligands in **1** (1462, 1224, and 1012 cm^{-1}) are not observed in the spectrum of HL; the same concerns a broad ν (H$_2$O) band at ~3400 cm^{-1}.
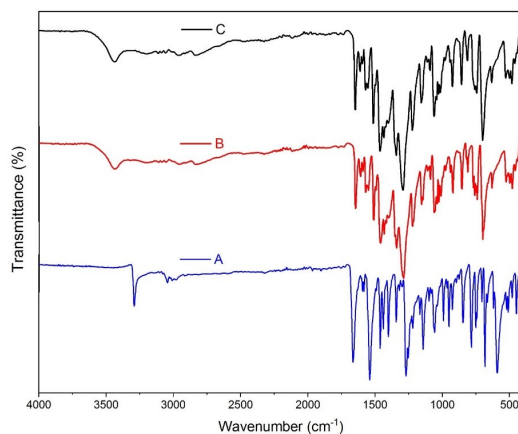

Figure 4. FT-IR spectra of (**A**) HL, (**B**) single crystals of **1**, and (**C**) nanoparticles of **1**.

TGA of a microcrystalline sample of **1** (Fig. S5) shows a weight variation compatible with the release of two water molecules (water ligand and crystallization solvent) in the 125−170 °C range (exp. 3.8%; calcd. 4.0%). After this temperature, a multistep decomposition of the sample begins. It is essentially complete at 490 °C, revealing the formation of CdO, as attested by a remaining weight of the sample (exp. 28.8%; calcd. 28.6%).

3.4. Characterization of Nanoparticles of **1** and CdO

Nanoparticles of the 1D coordination polymer **1** were prepared using the sonochemical method. The reaction parameters (molar ratio of the reagents and solvent) of the sonochemical reaction were

similar to those of the branched tube method that was used to obtain single crystals of **1**. Similarities between the reaction parameters permitted us to minimize the formation of impurities. In addition to identical FT-IR spectra of the single crystals and nanoparticles of **1**, their PXRD patterns are also similar. Their comparison with a pattern simulated from the single crystal data (Figure 5) indicates that there is only one crystalline phase in the obtained samples.
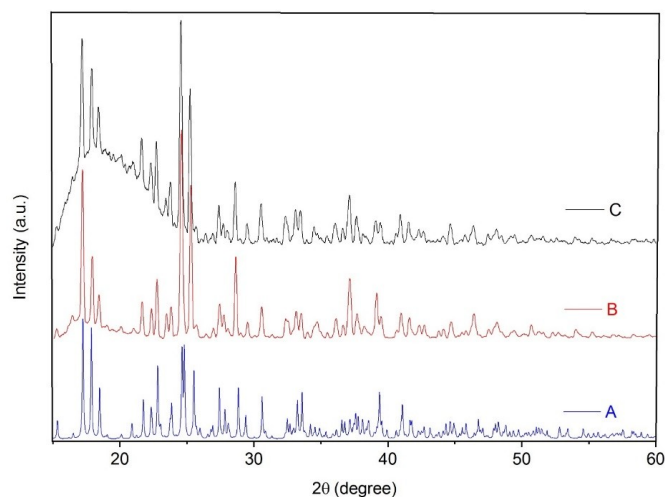
Figure 5. Powder X-ray diffraction patterns of coordination polymer **1**: (**A**) simulated from single crystal X-ray data, (**B**) prepared via a branched tube method, and (**C**) prepared by a sonochemical synthesis.

The size and morphology of the nanostructured coordination polymer **1** were studied by TEM (transmission electron microscopy). TEM images of the particles indicate their spherical morphology with the diameter distribution of 30−150 nm (Figure 6 and Figure S6). No significant change in the size and morphology of the particles was detected on adjusting the sonochemical reaction parameters, such as reaction time, and a molar ratio of the reagents. However, solvent (EtOH) appears to have an important effect in achieving the sonochemical synthesis of **1**, since PXRD patterns and FT-IR spectra of a solid formed as a result of similar sonochemical reaction in methanol instead of ethanol were totally different from the data of **1**, thus revealing the formation of structurally different compound (Figures S7 and S8). A branched tube method using methanol as the solvent did not lead to the formation of single crystals suitable for X-ray diffraction.
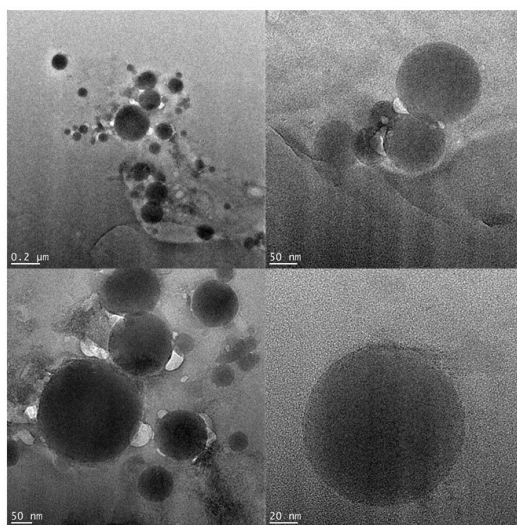
Figure 6. TEM images of nanospheres of coordination polymer **1** (sonochemical synthesis).

Nanospheres of CdO were prepared by the thermolysis of nanospheres of **1** at 500 °C in the presence of oleylamine as a surfactant (Figure 7). PXRD pattern of the synthesized CdO nanoparticles well matches the standard pattern of cubic CdO (ICDD 05-0640), thus confirming the formation of a pure phase. Major peaks in the PXRD pattern can be indexed as (111), (200), (220), (311), and (222) planes (Figure 8). TEM images of the prepared CdO nanoparticles show a uniform spherical morphology with an average diameter of 10 nm (Figure 7 and Figure S6).
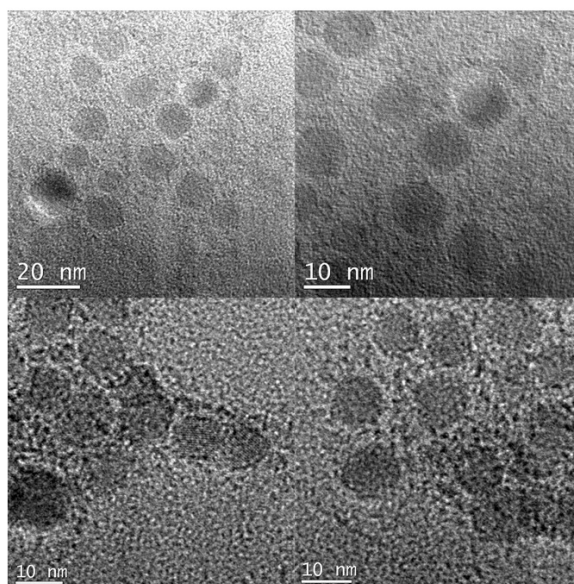

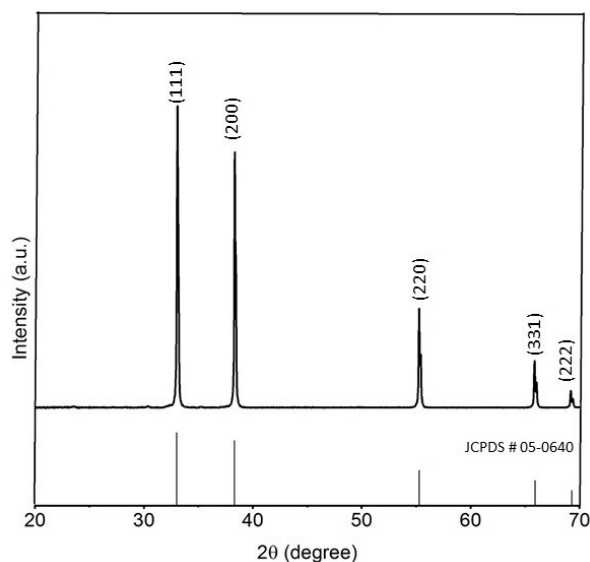**Figure 7.** TEM images of the nanospheres of CdO.

Figure 8. PXRD pattern of CdO nanospheres.

4. Conclusions

In this study, we have shown that a facile sonochemical method can be very efficient for the generation of a new 1D coordination polymer $\{[Cd_2(\mu\text{-}HL)(\mu\text{-}L)(NO_3)_3(H_2O)]\cdot H_2O\}_n$ (**1**), which is driven by pyridine-2-carboxaldehyde isonicotinoyl hydrazone. This method not only complements a branched tube technique for the assembly of single crystals of **1,** but it also allows for the generation of this coordination polymer in the form of nanoparticles. Both methods result in good product yields

and phase purity; the obtained samples are essentially equal, as confirmed by elemental analysis, FT-IR spectroscopy, and PXRD analyses.

Single-crystal X-ray structure of **1** was determined and analyzed in detail, revealing the formation of interdigitated tooth-shaped 1D metal-organic chains that are further extended (1D→3D) to an intricate hydrogen-bonded network. Topological analysis of this 3D network was performed, featuring a very rare **hms** (3,5-conn) underlying net. The sonochemically generated nanoparticles of **1** act as precursors for the synthesis of CdO nanospheres (cubic CdO) by thermolysis and in the presence of surfactant. Uniform spherical morphology of both coordination polymer **1** and CdO was confirmed by TEM.

In summary, this work widens the application of sonochemical synthetic methods for the generation of nanoparticles, coordination polymers, and derived products. This work also shows that such a synthetic methodology can be accomplished within a short period of time, and by using ethanol as a green and renewable solvent. Further research will be pursued on extending the application of sonochemical synthetic protocols to broaden the family of hydrazone-driven coordination polymers and related nanomaterials.

Supplementary Materials: The following materials are available online at http://www.mdpi.com/2073-4352/9/4/199/s1: H-bond parameters (Table S1), additional figures (Figures S1−S8) and crystal structure of **1** in CIF format (CCDC 1885947).

Conflicts of Interest: The authors declare no conflicts of interest.

References

1. Visakh, P.M.; Morlanes, M.J.M. (Eds.) *Nanomaterials and Nanocomposites: Zero- to Three-Dimensional Materials and Their Composites*; John Wiley & Sons: Hoboken, NJ, USA, 2016.
2. Vollath, D. *Nanomaterials: An Introduction to Synthesis, Properties and Applications*; John Wiley & Sons: Hoboken, NJ, USA, 2013.
3. Kharisov, B.I.; Kharissova, O.V.; Ortiz-Mendez, U. *Handbook of Less-Common Nanostructures*; CRC Press: Boca Raton, FL, USA, 2012.
4. Fan, Z.; Zhang, H. Crystal phase-controlled synthesis, properties and applications of noble metal nanomaterials. *Chem. Soc. Rev.* **2016**, *45*, 63–82. [CrossRef] [PubMed]
5. Raza, M.A.; Kanwal, Z.; Rauf, A.; Sabri, A.N.; Riaz, S.; Naseem, S. Size- and Shape-Dependent Antibacterial Studies of Silver Nanoparticles Synthesized by Wet Chemical Routes. *Nanomaterials* **2016**, *6*, 74. [CrossRef]
6. Shen, X.-F.; Yan, X.P. Facile shape-controlled synthesis of well-aligned nanowire architectures in binary aqueous solution. *Angew. Chem. Int. Ed.* **2007**, *46*, 7659–7663. [CrossRef] [PubMed]
7. Tan, C.-S.; Hsu, S.-C.; Ke, W.-H.; Chen, L.-J.; Huang, M.H. Facet-Dependent Electrical Conductivity Properties of Cu_2O Crystals. *Nano Lett.* **2015**, *15*, 2155–2160. [CrossRef]
8. Liu, P.; Qin, R.; Fu, G.; Zheng, N. Surface Coordination Chemistry of Metal Nanomaterials. *J. Am. Chem. Soc.* **2017**, *139*, 2122–2131. [CrossRef]
9. Peng, W.; Qu, S.; Cong, G.; Wang, Z. Synthesis and Structures of Morphology-Controlled ZnO Nano- and Microcrystals. *Cryst. Growth Des.* **2006**, *6*, 1518–1522. [CrossRef]
10. Han, W.; Yi, L.; Zhao, N.; Tang, A.; Gao, M.; Tang, Z. Synthesis and Shape-Tailoring of Copper Sulfide/Indium Sulfide-Based Nanocrystals. *J. Am. Chem. Soc.* **2008**, *130*, 13152–13161. [CrossRef]
11. Mirzaei, A.; Neri, G. Microwave-assisted synthesis of metal oxide nanostructures for gas sensing application: A review. *Sens. Actuators B* **2016**, *237*, 749–775. [CrossRef]

12. Li, C.; Yang, J.; Yang, P.; Lian, H.; Lin, J. Hydrothermal Synthesis of Lanthanide Fluorides LnF3 (Ln = La to Lu) Nano-/Microcrystals with Multiform Structures and Morphologies. *Chem. Mater.* **2008**, *20*, 4317–4326. [CrossRef]

13. Mehta, J.P.; Tian, T.; Zeng, Z.; Divitini, G.; Connolly, B.M.; Midgley, P.A.; Tan, J.-C.; Fairen-Jimenez, D.A.; Wheatley, E.H. Sol–Gel Synthesis of Robust Metal–Organic Frameworks for Nanoparticle Encapsulation. *Adv. Funct. Mater.* **2018**, *28*, 1705588. [CrossRef]

14. Blin, J.-L.; Stébé, M.-J.; Lebeau, B. Hybrid/porous materials obtained from nano-emulsions. *Curr. Opin. Colloid. Interfaces Sci.* **2016**, *25*, 75–82. [CrossRef]

15. Chhatre, A.; Duttagupta, S.; Thaokar, R.; Mehra, A. Mechanism of Nanorod Formation by Wormlike Micelle-Assisted Assembly of Nanospheres. *Langmuir* **2015**, *31*, 10524–10531. [CrossRef]

16. Moulik, S.P.; De, G.C.; Panda, A.K.; Bhowmik, B.B.; Das, A.R. Dispersed Molecular Aggregates. 1. Synthesis and Characterization of Nanoparticles of $Cu_2[Fe(CN)_6]$ in H_2O/AOT/n-Heptane Water-in-Oil Microemulsion Media. *Langmuir* **1999**, *15*, 8361–8367. [CrossRef]

17. Thanh, N.T.K.; Maclean, N.; Mahiddine, S. Mechanisms of Nucleation and Growth of Nanoparticles in Solution. *Chem. Rev.* **2014**, *114*, 7610–7630. [CrossRef]

18. Ameta, S.C.; Ameta, R.; Ameta, G. (Eds.) *Sonochemistry: An Emerging Green Technology*; CRC Press: Boca Raton, FL, USA, 2018.

19. Colmenares, J.C.; Chatel, G. (Eds.) *Sonochemistry: From Basic Principles to Innovative Applications*; Springer: Berlin, Germany, 2017.

20. Abdolalian, P.; Morsali, A.; Bruno, G. Sonochemical synthesis and characterization of microrod to nanoparticle of new mixed-ligand zinc(II) fumarate metal-organic polymer. *Ultrason. Sonochem.* **2017**, *37*, 654–659. [CrossRef]

21. Mousavi, S.A.; Montazerozohori, M.; Masoudiasl, A.; Mahmoudi, G.; White, J.M. Sonication-assisted synthesis of a new cationic zinc nitrate complex with a tetradentate Schiff base ligand: Crystal structure, Hirshfeld surface analysis and investigation of different parameters influence on morphological properties. *Ultrason. Sonochem.* **2018**, *46*, 26–35. [CrossRef]

22. Morsali, A.; Monfared, H.H.; Janiak, C. Ultrasonic irradiation assisted syntheses of one-dimensional di(azido)-dipyridylamine Cu(II) coordination polymer nanoparticles. *Ultrason. Sonochem.* **2015**, *23*, 208–211. [CrossRef]

23. Derakhshandeh, P.G.; Soleimannejad, J.; Janczak, J. Sonochemical synthesis of a new nano-sized cerium(III) coordination polymer and its conversion to nanoceria. *Ultrason. Sonochem.* **2015**, *26*, 273–280. [CrossRef]

24. Xu, H.; Zeiger, B.W.; Suslick, K.S. Sonochemical synthesis of nanomaterials. *Chem. Soc. Rev.* **2013**, *42*, 2555–2567. [CrossRef]

25. Safarifard, V.; Morsali, A. Applications of ultrasound to the synthesis of nanoscale metal–organic coordination polymers. *Coord. Chem. Rev.* **2015**, *292*, 1–14. [CrossRef]

26. Fillion, H.; Luche, J.L. *Synthetic Organic Sonochemistry*; Plenum Press: New York, NY, USA, 1998.

27. MacGillivray, L.R. (Ed.) *Metal-Organic Frameworks: Design and Application*; John Wiley & Sons: Hoboken, NJ, USA, 2010.

28. Sander, J.R.G.; Bucar, D.K.; Henry, R.F.; Zhang, G.G.Z.; MacGillivray, L.R. Pharmaceutical Nano-Cocrystals: Sonochemical Synthesis by Solvent Selection and Use of a Surfactant. *Angew. Chem., Int. Ed.* **2010**, *49*, 7284–7288. [CrossRef]

29. Kolhatkar, A.G.; Jamison, A.C.; Litvinov, D.; Willson, R.C.; Lee, T.R. Tuning the Magnetic Properties of Nanoparticles. *Int. J. Mol. Sci.* **2013**, *14*, 15977–16009. [CrossRef]

30. Miller, L.W.; Tejedor, M.I.; Nelson, B.P.; Anderson, M.A. Mesoporous Metal Oxide Semiconductor-Clad Waveguides. *J. Phys. Chem. B* **1999**, *103*, 8490–8492. [CrossRef]

31. Fernández, M.; Martínez, A.; Hanson, J.C.; Rodriguez, A.J. Nanostructured Oxides in Chemistry: Characterization and Properties. *Chem. Rev.* **2004**, *104*, 4063–4104. [CrossRef]

32. Jefferson, P.H.; Hatfield, S.A.; Veal, T.D.; King, P.D.C.; McConville, C.F. Bandgap and effective mass of epitaxial cadmium oxide. *Appl. Phys. Lett.* **2008**, *92*, 022101. [CrossRef]

33. Malik, M.A.; O'Brien, P. *Organometallic and Metallo-Organic Precursors for Nanoparticles Precursor Chemistry of Advanced Materials*; Fischer, R., Ed.; Springer: Berlin/Heidelberg, Germany, 2005; p. 173.

34. Leong, W.L.; Vittal, J.J. One-Dimensional Coordination Polymers: Complexity and Diversity in Structures, Properties, and Applications. *Chem. Rev.* **2010**, *111*, 688–764. [CrossRef]

35. Vittal, J.J.; Ng, M.T. Chemistry of Metal Thio- and Selenocarboxylates: Precursors for Metal Sulfide/Selenide Materials, Thin Films, and Nanocrystals. *Acc. Chem. Res.* **2006**, *39*, 869–877. [CrossRef]

36. Masoomi, M.Y.; Morsali, A. Applications of metal–organic coordination polymers as precursors for preparation of nano-materials. *Coord. Chem. Rev.* **2012**, *256*, 2921–2943. [CrossRef]

37. Mahmoudi, G.; Stilinović, V.; Bauzá, A.; Frontera, A.; Bartyzel, A.; Ruiz-Pérez, C.; Kirillov, A.M. Inorganic–organic hybrid materials based on PbBr2 and pyridine–hydrazone blocks – structural and theoretical study. *RSC Adv.* **2016**, *6*, 60385–60393. [CrossRef]

38. Mahmoudi, G.; Khandar, A.A.; White, J.; Mitoraj, M.P.; Jena, H.S.; Van Der Voort, P.; Qureshi, N.; Kirillov, A.M.; Robeynsi, K.; Safin, D.A. Polar protic solvent-trapping polymorphism of the HgII-hydrazone coordination polymer: experimental and theoretical findings. *CrystEngComm* **2017**, *19*, 3017–3025. [CrossRef]

39. Huang, W.; Jiang, J.; Wu, D.; Xu, J.; Xue, B.; Kirillov, A.M. A Highly Stable Nanotubular MOF Rotator for Selective Adsorption of Benzene and Separation of Xylene Isomers. *Inorg. Chem.* **2015**, *54*, 10524–10526. [CrossRef]

40. Iqbal, K.; Iqbal, A.; Kirillov, A.M.; Liu, W.; Tang, Y. Hybrid Metal–Organic-Framework/Inorganic Nanocatalyst toward Highly Efficient Discoloration of Organic Dyes in Aqueous Medium. *Inorg. Chem.* **2018**, *57*, 13270–13278. [CrossRef]

41. Gu, J.-Z.; Cai, Y.; Wen, M.; Shi, Z.-F.; Kirillov, A.M. A New Series of Cd(II) Metal–Organic Architectures Driven by Soft Ether-Bridged Tricarboxylate Spacers: Synthesis, Structural and Topological Versatility, and Photocatalytic Properties. *Dalton Trans.* **2018**, *47*, 14327–14339. [CrossRef]

42. Gu, J.-Z.; Cui, Y.-H.; Liang, X.-X.; Wu, J.; Lv, D.; Kirillov, A.M. Structurally Distinct Metal-Organic and H-bonded Networks Derived from 5-(6-Carboxypyridin-3-yl)isophthalic Acid: Coordination and Template Effect of 4,4′-Bipyridine. *Cryst. Growth Des.* **2016**, *16*, 4658–4670. [CrossRef]

43. Fernandes, T.A.; Santos, C.I.M.; André, V.; Kłak, J.; Kirillova, M.V.; Kirillov, A.M. Copper(II) Coordination Polymers Self-assembled from Aminoalcohols and Pyromellitic Acid: Highly Active Pre-catalysts for the Mild Water-promoted Oxidation of Alkanes. *Inorg. Chem.* **2016**, *55*, 125–135. [CrossRef] [PubMed]

44. Gu, J.-Z.; Wen, M.; Liang, X.; Shi, Z.-F.; Kirillova, M.V.; Kirillov, A.M. Multifunctional Aromatic Carboxylic Acids as Versatile Building Blocks for Hydrothermal Design of Coordination Polymers. *Crystals* **2018**, *8*, 83. [CrossRef]

45. Rasband, W.S. *ImageJ.*; U.S. National Institutes of Health: Bethesda, MD, USA, 1997–2016.

46. *Bruker Saint Plus*; Saint Plus 8.34A; Bruker AXS Inc.: Madison, WI, USA, 2007.

47. *Bruker SADABS, TWINABS, SADABS 2012/1*; Bruker AXS Inc.: Madison, WI, USA, 2001.

48. Sheldrick, G.M. Crystal structure refinement with SHELXL. *Acta. Cryst.* **2015**, *C71*, 3–8.

49. Sheldrick, G.M. A short history of SHELX. *Acta Cryst.* **2008**, *A64*, 112–122. [CrossRef] [PubMed]

50. Hübschle, C.B.; Sheldrick, G.M.; Dittrich, B.J. ShelXle: A Qt graphical user interface for SHELXL. *Appl. Cryst.* **2011**, *44*, 1281–1284. [CrossRef] [PubMed]

51. Macrae, C.F.; Bruno, I.J.; Chisholm, J.A.; Edgington, P.R.; McCabe, P.; Pidcock, E.; Rodriguez-Monge, L.; Taylor, R.; van de Streek, J.; Wood, P.A. Mercury CSD 2.0–new features for the visualization and investigation of crystal structures. *J. Appl. Cryst.* **2008**, *41*, 466–470. [CrossRef]

52. Blatov, V.A. Multipurpose crystallochemical analysis with the program package TOPOS. *IUCr Comp. Comm. Newslett.* **2006**, *7*, 4–38.

53. Blatov, V.A.; Shevchenko, A.P.; Proserpio, D.M. Applied Topological Analysis of Crystal Structures with the Program Package ToposPro. *Cryst. Growth Des.* **2014**, *14*, 3576–3586. [CrossRef]

54. Richardson, D.R.; Becker, E.; Bernhardt, P.V. The biologically active iron chelators 2-pyridylcarboxaldehyde isonicotinoylhydrazone, 2-pyridylcarboxaldehyde benzoylhydrazone monohydrate and 2-furaldehyde isonicotinoylhydrazone. *Acta Crystallogr.* **1999**, *C55*, 2102–2105. [CrossRef]

55. Yumnam, S.; Rajkumari, L. Thermodynamics of the Complexation of N-(Pyridin-2-ylmethylene) Isonicotinohydrazide with Lighter Lanthanides. *J. Chem. Eng. Data* **2009**, *54*, 28–34. [CrossRef]

56. Khandar, A.A.; Afkhami, F.A.; Yazdi, S.A.H.; White, J.M.; Kassel, S.; Dougherty, W.G.; Lipkowski, J.; Van Derveer, D.; Giester, G.; Costantino, F. Anion influence in the structural diversity of cadmium coordination polymers constructed from a pyridine based Schiff base ligand. *Inorg. Chim. Acta* **2015**, *427*, 87–96. [CrossRef]

57. Khandar, A.A.; Ghosh, B.K.; Lampropoulos, C.; Gargari, M.S.; Yilmaz, V.T.; Bhar, K.; Yazdi, S.A.H.; Cain, J.M.; Mahmoudi, G. Coordination complexes and polymers from the initial application of phenyl-2-pyridyl ketone azine in mercury chemistry. *Polyhedron* **2015**, *85*, 467–475. [CrossRef]

58. Huang, J.-H.; Hou, G.-F.; Ma, D.-S.; Yu, Y.-H.; Jiang, W.-H.; Huang, Q.; Gao, J.-S. Two pairs of Zn(II) coordination polymer enantiomers based on chiral aromatic polycarboxylate ligands: synthesis, crystal structures and properties. *RSC Adv.* **2017**, *7*, 18650–18657. [CrossRef]

59. An, Y.-Y.; Lu, L.-P.; Zhu, M.-L. A three-dimensional twofold interpenetrated cobalt(II) MOF containing a flexible carboxylate-based ligand: synthesis, structure and magnetic properties. *Acta Cryst.* **2018**, *C74*, 418–423.